

## DESIGN OF MIMO ANTENNA FOR WIRELESS COMMUNICATION APPLICATIONS

\*Rasha Basil Nassir

Ali Khalid Jassim

Electrical Engineering Department, College of Engineering, Mustansiriya University, Baghdad, Iraq

Received 16/12/2021

Accepted in revised form 17/2/2022

Published 1/7/2022

**Abstract:** The development of a new compact Ultra Wideband (UWB) antenna. The main advantages of the proposed array configuration are that it requires no isolation/decoupling circuit between the elements of the MIMO array. The suggested antenna has an impedance bandwidth of (3.1\_10.6) GHz. The antenna dimension (25×58×1.6) mm<sup>3</sup>. It is based on a simple patch antenna configuration with a simple hexagonal radiator and partial ground. The partial ground is used to improve the reflection coefficient and isolation. A 16.54mm x 9mm ground plane is used. Each element was fed through a 50Ω microstrip transmission line (MTL). The suggested antenna is polarized linearly. It performs admirably at 10.46 GHz, with a gain of 1.77dB, a reflection coefficient of 28.42dB, VSWR approx 1, an envelope correlation coefficient very close to 0 dB, a diversity gain of 10dB, and isolation of 50.44dB, respectively, and suggested antenna's diversity characteristics, such as ECC and diversity gain, are also modeled.

**Keywords:** *Wideband antennas, UWB antennas, mutual coupling, MIMO antenna, envelope correlation coefficient, high isolation, microstrip antenna.*

### 1. Introduction

Wireless communication systems must be capable of handling massive amounts of data while maintaining a high level of service quality. Due to its high throughput and low power spectral density, ultra wideband (UWB) technology is viewed as promising for short-

range communication applications such as personal area networks. On the other hand, It Modern faces reliability and multipath fading concerns, which are much more prevalent in personal area network (PAN) applications [1]. By comparison, the multiple-input multiple-output (MIMO) technique has long been considered the optimal solution for the vast majority of problems encountered in wireless communication systems [2]. Thus, by combining UWB and MIMO technologies, data throughput is increased while multipath issues are minimized [3]. Correlation and mutual coupling between antennas must be minimized to maximize the MIMO technology's effectiveness in an antenna system. . However, as the number of antenna elements on space-constrained portable devices increases, the spacing between them decreases, resulting in extremely strong mutual coupling. As a result, the primary challenge in designing a compact planar UWB MIMO antenna array is to maximize the number of components in the array while maintaining high isolation and avoiding the use of decoupling and matching circuits in space-constrained

\*Corresponding Author: [Eema1016@uomustansiriyah.edu.iq](mailto:Eema1016@uomustansiriyah.edu.iq)

portable wireless devices. Numerous previous publications have described numerous UWB MIMO antenna designs. Numerous articles [4], [5], [6] discuss how to improve isolation by utilizing a variety of matching and decoupling circuits of various designs and structures. While the majority of articles assert that aligning orthogonal elements results in inherent isolation, they all rely on some form of decoupling circuit to accomplish this. [4-9]. To increase channel capacity and reliability at the same time, a system's antenna elements must be greater than two. Only a few articles have described topologies for four-element UWB MIMO antenna arrays, and none of them support both small size and easy element expansion without requiring any decoupling or isolating structure [3]. The array must be easily extensible in order to meet the design requirements of future wireless communication systems.

Numerous studies have been carried out to determine a single, dual and narrower band MIMO array with high isolation and small size. The authors of references [11-17] have designed a single, dual and narrower band with high isolation and small size for wireless communication applications. In reference [11], the size of the antenna that was used to design is  $(100 \times 50) \text{ mm}^2$ , the band obtained from this design is (3.4\_3.6) GHz, and the isolation is 10dB. In reference [12], the size that is used to design the antenna is  $(136 \times 68) \text{ mm}^2$ , the band obtained from this design is (3.4\_3.6) GHz, and the isolation is 15dB. In reference [13], the size that is used to design the antenna is  $(150 \times 75) \text{ mm}^2$ , the band obtained from this design is (3.55\_3.65) GHz, and the isolation is 11dB. In reference [14], the size of the antenna is  $(41.3 \times 46) \text{ mm}^2$  and the resonance frequency is 28 GHz. In reference [15], the size of the antenna is  $(220 \times 320) \text{ mm}^2$ , the bandwidth obtained from this design is 84 MHz, 200MHz. In reference

[16], the size of the antenna is  $(120 \times 65) \text{ mm}^2$ , the bandwidth is 1.7GHz, the value of isolation  $>18.8\text{dB}$ , and the value of  $\text{ECC} < 0.018$ . In reference [17], the size of the antenna is  $(150 \times 150) \text{ mm}^2$ ; the bandwidth is 85MHz, the type of decoupling technique is EBG, the maximum isolation improvement obtained from this design is 20dB.

The purpose of this article is to discuss a  $58\text{mm} \times 25\text{mm}$  single-band MIMO array with a high return loss and good isolation. The MIMO antenna is constructed from two hexagonal elements connected via a rectangular microstrip. The partial ground enhances the antenna performance, whereas the joint ground degrades it. Two symmetrical elements comprise the antenna, one of which is partially grounded. The partial ground has an effect on current distribution and decreases inter-element coupling, increasing isolation.

This work is structured in the following manner: section 2 examined the MIMO array's design.; section 3 studied the result, discussion, and comparison with published work; section 4 represented a short conclusion.

## **2. Antenna Design**

Figure 2 illustrates the final UWB MIMO antenna geometry because the design of Figure 1 is not suitable to use due to the value of  $S_{11}$  isn't less than  $-10\text{dB}$ . The suggested design was printed on an FR\_4 substrates with dimensions of  $(25 \times 58 \times 1.6) \text{ mm}^3$ , a relative permittivity of  $\epsilon_r = 4.3$ , and a loss tangent of 0.025. The antenna is composed of two hexagonal radiation patches at the dielectric substrate's top, as well as two partial ground. The partial ground is employed to increase the reflection coefficient and decrease the coupling between the antenna's elements. Each patch of the MIMO array has a single feedline. The antenna is designed in two ways, with the total size of the antenna remaining

constant throughout. This section discusses the evolution of the proposed design, including the UWB antenna element and the antenna's ground structure.

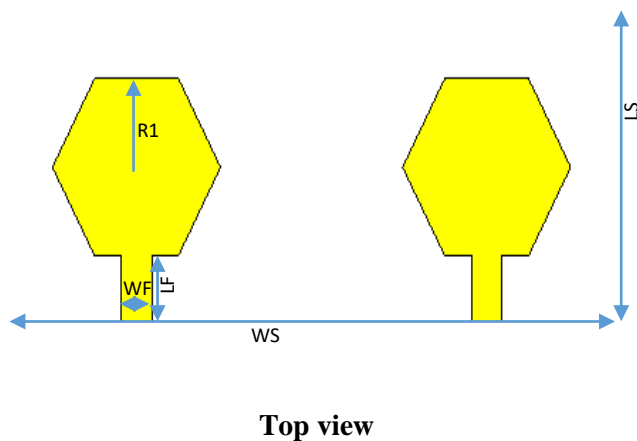
Additionally, all measurements are listed in Table1, which is highlighted in Figure 2 and Figure1.

**Table 1.** Parameters for antenna design.

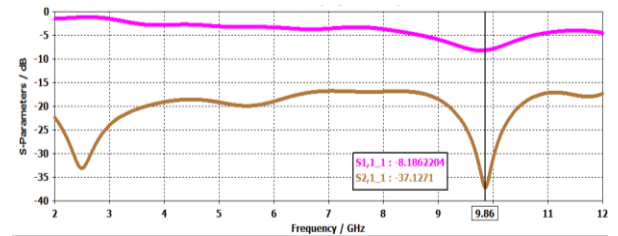
Parameters	Value (mm2)	Parameters	Value (mm2)
WG1	29	H	1.6
WS	58	T	0.035
LG	9	WF	2.93
LF	5.51	LS	25
R1	8	WG2	16.54
G	4		

The following is a brief explanation of comparison between the two ways that used to design antenna:

First way: the MIMO consists of two elements connected by common ground. Each patch of the array is connected with a single feedline. The configuration of the array, the reflection coefficient, and the coupling of this way are illustrated in Figure1. This way is not used in my paper because the S11 is not less than -10dB.



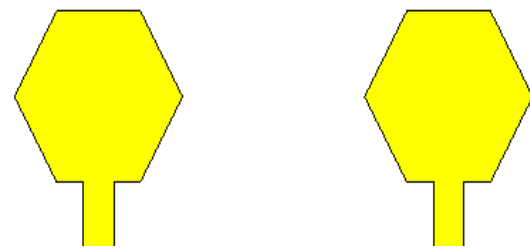
**Back view**  
(a)



(b)

**Figure 1.** A simulated two-element array setup was similar to the one used in a first way. (a) the shape of the MIMO with front and back views. (b) coefficient of reflection and transmission among the first and second elements.

Second way: the suggested antenna is composed of two elements; every element has a separate ground; in order to improve the antenna's performance over the first way. This way is dependent on my paper because the value of S11 in this way is less than -10dB. It should be noted that each patch is connected with a single feedline. The configuration of the array, the reflection coefficient, and the coupling of this way are illustrated in Figure 2.



**Front view**

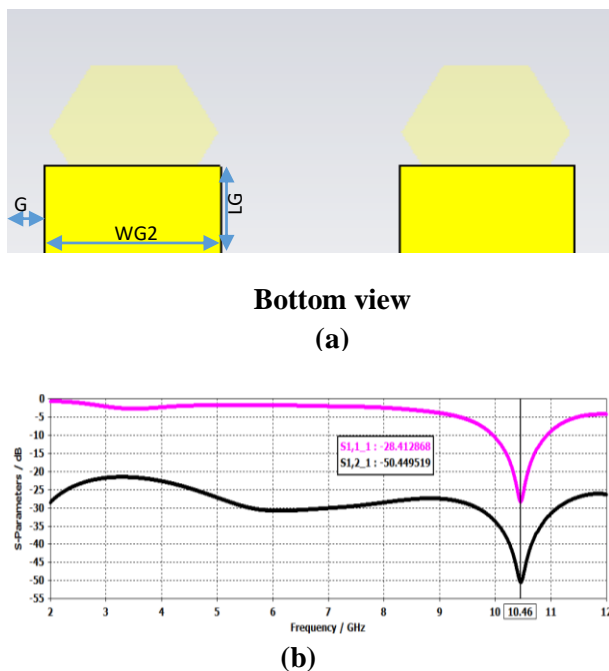


**Figure 2.** A simulated two-element array setup was similar to the one used in a second way. (a) the shape of the array from front and back views. (b) coefficient of reflection and transmission among the first and second elements.

### 3. Results and Discussions

The simulation section uses CST. STUDIO 2020 to determine performance characteristics such as return losses  $S_{nm}$ , mutual coupling  $S_{jk}$ , radiation pattern, envelop correlation coefficient (ECC), diversity gain (DG), and voltage standing wave ratio (VSWR). In Figure 2(a), the left element is referred to as antenna I, while the second element is referred to as antenna II. The maximum power transfer (matching the feedline to the antenna's input impedance) can be considered the most critical parameter, where  $S_{11}$  represents the ratio of energy sent to energy reflected. As a result, the input reflection coefficient curve is a graph of an antenna's  $S_{11}$  versus frequency, as illustrated in figure2. The value of  $S_{11}$  of the proposed antenna will be  $-28.41\text{dB}$ . The value of  $S_{11}$  is equal to the value of  $S_{22}$ , so mentioned only the value of  $S_{11}$ . Due to the symmetrical structure of  $S_{12}$  and  $S_{21}$ , they are equivalent, and both

indicate the coupling coefficient between two antennas. The value of  $S_{21}$  of the proposed antenna will be  $-50.45\text{dB}$ . The  $S_{11}$  and  $S_{22}$  are smaller than  $10\text{dB}$  in the UWB frequency range, resulting in improved impedance matching performance for each independent antenna without a decoupling network; the suggested antenna's maximum coupling over the operating range is less than  $-20\text{ dB}$ , indicating that it is appropriate for MIMO applications in the UWB system. The surface current distribution experiment focused on the antenna components that affect the radiation characteristics and on revealing the amount of interaction between distinct MIMO antennas. The surface current distribution at operating frequencies of  $10.46\text{ GHz}$  is depicted in Figure3. The scale depicts the various colors, which are sorted in descending order according to the current value. The regions highlighted in red have a more favorable current distribution than the regions highlighted in yellow, green, and so on. Another important parameter describes the radiation properties of an antenna and distinguishes each antenna from the other, which is the pattern of radiation. Figure 4 illustrates the proposed antenna's simulated radiation patterns at operating frequencies of  $10.46\text{ GHz}$ . The antenna radiates bi directionally and omni directionally in the  $E = (0^\circ)$  and  $H = (90^\circ)$  planes, respectively.

Gain is defined as an antenna's ability to concentrate radiated power in a particular direction or, conversely, to effectively absorb incident power from that direction. The suggested antenna's gain is depicted in Figure 5. The gain will be greater than  $1.77\text{dB}$  over the operating band. The envelope correlation coefficient (ECC) is the primary design parameter for MIMO antennas; it quantifies the correlation between each pair of ports. A MIMO antenna should have a low ECC to indicate that the channels are independent. The proposed antenna's envelope correlation coefficient should be very small  $<0.5$  in order to produce great

diversity between the two elements. The diversity gain must be >9dB. The ECC is calculated as follows [10] using the far-field radiation pattern.

$$\rho_e = \frac{|\iint_{4\pi} \vec{F}_1(\theta, \phi) * \vec{F}_2(\theta, \phi) d\Omega|^2}{\iint_{4\pi} |\vec{F}_1(\theta, \phi)|^2 d\Omega \iint_{4\pi} |\vec{F}_2(\theta, \phi)|^2 d\Omega} \quad (1)$$

Where  $\vec{F}_i(\theta, \phi)$  denotes the MIMO antenna's far-field property after all ports have been excited. Figure6 illustrates the ECC calculated over the operational band, which appears to be quite close to 0dB. The calculating DG over the working band, which is approximately 10dB, is shown in Figure7.

$$DG = 10\sqrt{1 - ECC^2} \quad (2)$$

Figure8 illustrates the real and imaginary impedance. To achieve the best matching, the real impedance of the ideal antenna should be approximately 50, and the imaginary impedance should be approximately zero. The real portion of the simulation two-port antenna is approximately (48.32), while the imaginary portion is approximately (-3.32); these are both acceptable values that are close to the ideal state.

The voltage standing wave ratio (VSWR) for the microstrip antenna, which is designed at a frequency of 10.46GHz, is approximately equal to 1 and it is less than 2, so that the VSWR is "the ratio of maximum voltage or current to minimum voltage or current at any point it considers as a measure for the mismatch between the line and the load," and it is shown in Figure 9.

The VSWR and S11 are calculated using these equations:

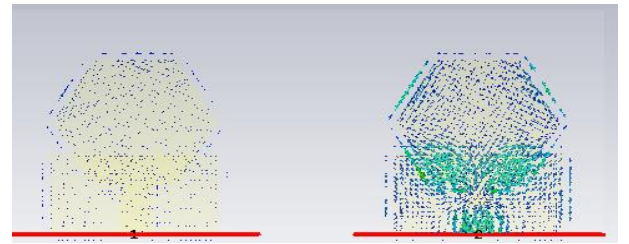
$$VSWR = \frac{V_{max}}{V_{min}} = \frac{1+\gamma}{1-\gamma} \quad (3)$$

Where  $\gamma$  represent the reflection coefficient

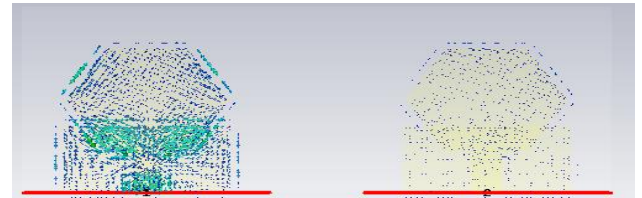
$$\gamma = \frac{Z_R - Z_0}{Z_R + Z_0} \quad (4)$$

And also

$$S11 = 10 \log \gamma \quad (5)$$

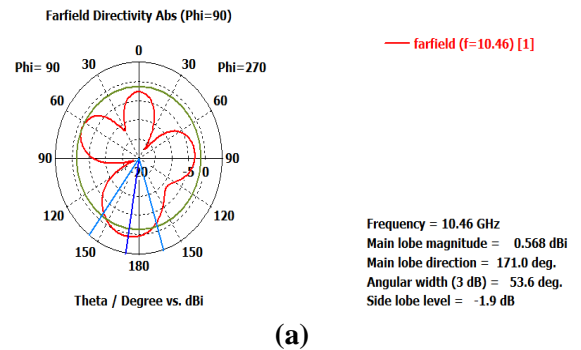


For the second element

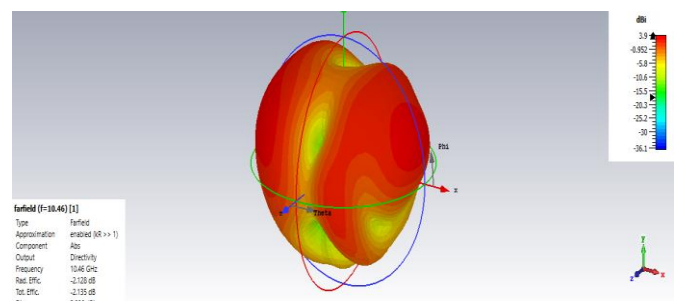


For the first element

Figure 3. Distribution of surface current at 10.46GHz.



(a)



(b)

Figure 4. Simulated radiation patterns (a) in one dimension and (b) in three dimensions.

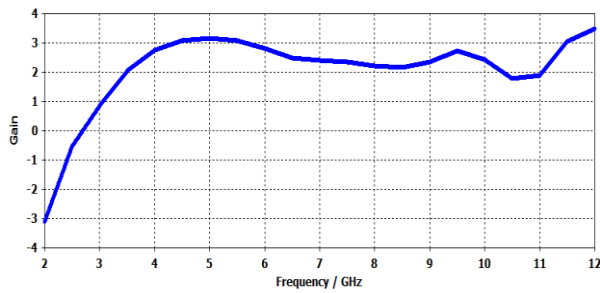


Figure 5. The suggested antenna's simulated gain.



Figure 6. The suggested antenna's envelope correlation coefficient.

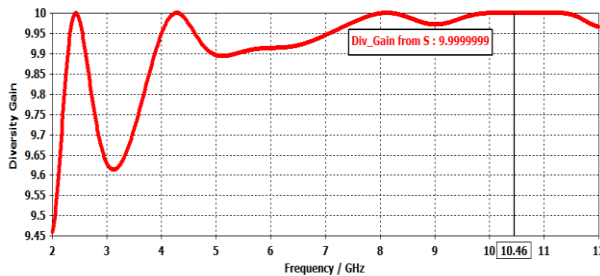


Figure 7. The suggested antenna's diversity gain.

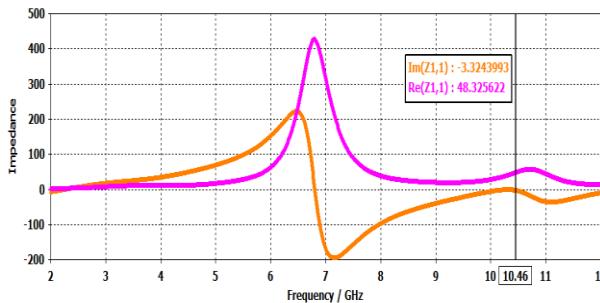


Figure 8. The proposed antenna's real and imaginary impedances.

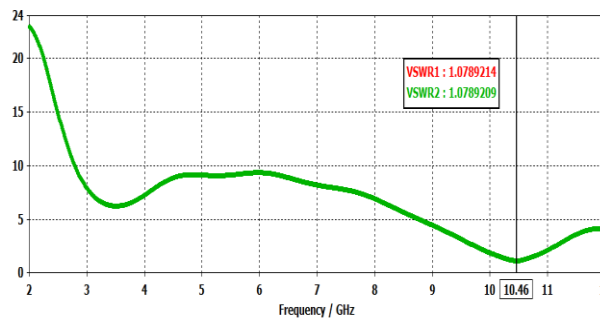


Figure 9. The suggested antenna's voltage standing wave ratio.

In accordance with the FCC judgments, UWB system can be defined as any system which is transmitting scheme that fill a fractional bandwidth (FBW) at least 0.2 or an absolute bandwidth at least 500MHz according to the following equation [18]:

$$FBW = 2 \frac{f_H - f_L}{f_H + f_L} \tag{6}$$

Where  $f_H$  and  $f_L$  are the upper edge and lower edge of bandwidth respectively.

This finding indicates that the suggested antenna array is capable of practical MIMO operation and can be utilized as a building block in the future to develop a MIMO array with four or more antennas.

Table 2. Comparison to previously published works.

Reference	Antenna Size (mm <sup>2</sup> )	Bandwidth h (GHz)	Isolation (dB)
[11]	100 × 50	3.4_3.6	10
[12]	136 × 68	3.4_3.6	15
[13]	150 × 75	3.55_3.65	11
My work	25 × 58	9.9608–10.9311	50.44

#### 4. Conclusions

This paper proposes a single printed MIMO antenna solution for use with UWB. The MIMO antenna system was created for UWB applications. It consists of two hexagon elements, each fed by a 50 microstrip transmission line (MTL) for impedance matching. Channel isolation was sufficient for MIMO operation. Despite this, the ground partial was used to increase the input reflection coefficient and isolation between the antenna parts. The proposed antenna works between 9.9608 and 10.9311 GHz. The bandwidth of the proposed antenna is 970.3 MHz exceeding 500MHz, so it considers UWB application. The hexagon-shaped MIMO antennas have a minimum isolation level of 50.44 dB throughout the bands of operating. The value of VSWR is approximately 1, and the value of S11 is -

28.41dB. The performance of the hexagon-shaped antenna in an isotropic environment was evaluated using the ECC, DG parameters. The ECC has been set near to 0dB for the 9.9608–10.9311 GHz bands of operating. These results indicate that the systems exhibit superior antenna characteristics, including constant gain under omnidirectional radiation, diversity, and multiplexing capability for MIMO operation.

### Acknowledgment

The authors wish to express their gratitude to Mustansiriyah university for its support of scientific research efforts.

### Conflict of interest

The authors confirm that there is no conflict of interest associated with the publication of this article.

### 5. References

1. L. Liu, S. W. Cheung, and T. I. Yuk, "Compact MIMO antenna for portable devices in UWB applications," *IEEE Trans. Antennas Propag.*, vol. 61, no. 8, pp. 4257–4264, Aug. 2013.
2. A. J. Paulraj, D. A. Gore, R. U. Nabar, and H. Bolcskei, "An overview of MIMO communications—A key to gigabit wireless," *Proc. IEEE*, vol. 92, no. 2, pp. 198–218, Feb. 2004.
3. X.-Liu, Z.-Wang, Y.-Yin, J. Ren, and J.-Wu, "A compact ultrawideband MIMO antenna using QSCA for high isolation," *IEEE Antennas Wireless Propag. Lett.*, vol. 13, pp. 1497–1500, 2014.
4. Ullah, U.; Al-Hasan, M.; Koziel, S.; Mabrouk, I.B. Circular Polarization Diversity Implementation for Correlation Reduction in Wideband Low-Cost Multiple-Input-Multiple-Output Antenna. *IEEE Access* 2020, 8, 95585–95593.
5. Li, Z.; Yin, C.; Zhu, X. Compact UWB MIMO Vivaldi Antenna with Dual Band-Notched Characteristics. *IEEE Access* 2019, 7, 38696–38701.
6. Kumar, P.; Urooj, S.; Alrowais, F. Design and Implementation of Quad-Port MIMO Antenna with Dual-Band Elimination Characteristics for Ultra-Wideband Applications. *Appl. Sci.* 2020, 10, 1715.
7. Iqbal, A.; A Saraereh, O.; Bouazizi, A.; Basir, A. Metamaterial-Based Highly Isolated MIMO Antenna for Portable Wireless Applications. *Electronics* 2018, 7, 267.
8. Zhu, J.; Li, S.; Liao, S.; Xue, Q. Wideband Low-Profile Highly Isolated MIMO Antenna with Artificial Magnetic Conductor. *IEEE Antennas Wirel. Propag. Lett.* 2018, 17, 458–462.
9. Chatterjee, J.; Mohan, A.; Dixit, V. Broadband Circularly Polarized H-Shaped Patch Antenna Using Reactive Impedance Surface. *IEEE Antennas Wirel. Propag. Lett.* 2018, 17, 625–628.
10. Sharawi, M.S. Printed MIMO Antenna Engineering; Artech House: Norwood, MA, USA, 2014.
11. Al-Hadi, A.A.; Ilvonen, J.; Valkonen, R.; Viikan, V. Eight-element antenna array for diversity and MIMO mobile terminal in LTE 3500MHz band. *Microw. Opt. Technol. Lett.* 2014, 56, 1323–1327.
12. Abdullah, M. Compact 4-Port MIMO antenna system for 5G mobile terminal. In Proceedings of the International Applied Computational Electromagnetics Society Symposium, Florence, Italy, 26–30 March 2017.
13. Ojaroudi Parchin, N.; Al-Yasir, Y.I.A.; Abd-Alhameed, R.A.; Noras, J.M. Dual-polarized MIMO antenna array design using miniaturized self-complementary structures for 5G smartphone applications. In Proceedings of the EuCAP Conference, Krakow, Poland, 31 March–5 April 2019.

14. Yoon, N.; Seo, C. A 28-GHz Wideband 2 × 2 U-Slot Patch Array Antenna. *J. Electromagn. Eng. Sci.* 2017, 17, 133–137.
15. Lee, C. T., Su, S. W., Chen, S. C. & Fu, C. S. Low-Cost, Direct-Fed Slot Antenna Built in Metal Cover of Notebook Computer for 2.4/5.2/5.8-GHz WLAN Operation. *IEEE Trans. Antennas Propag.* 65(5), 2677–2682 (2017).
16. A. Biswas and V. R. Gupta, “Design and development of low-profile MIMO antenna for 5G new radio smartphone applications,” *Wireless Personal Communications*, vol. 111, no. 3, pp. 1695–1706, 2020.
17. ZHAI, G., CHEN, Z. N., QING, X. Mutual coupling reduction of a closely spaced four-element MIMO antenna system using discrete mushrooms. *IEEE Transactions on Microwave Theory and Techniques*, 2016, vol. 64, no. 10, p. 3060–3067. DOI:10.1109/TMTT.2016.2604314
18. J. Liang, *Antenna Study and Design for UltraWideband Communication Applications*, Phd Thesis, University of London, United Kingdom, July 2006.